

We are IntechOpen, the world's leading publisher of Open Access books Built by scientists, for scientists

4,800

Open access books available

122,000

International authors and editors

135M

Downloads

Our authors are among the

154

Countries delivered to

TOP 1%

most cited scientists

12.2%

Contributors from top 500 universities



WEB OF SCIENCE™

Selection of our books indexed in the Book Citation Index
in Web of Science™ Core Collection (BKCI)

Interested in publishing with us?
Contact book.department@intechopen.com

Numbers displayed above are based on latest data collected.

For more information visit www.intechopen.com



Electron Oscillation-Based Mono-Color Gamma-Ray Source

Hai Lin, ChengPu Liu and Chen Wang

Abstract

Production of artificial gamma-ray source usually is a conception belonging to the category of experimental nuclear physics. Nuclear physicists achieve this goal through utilizing/manipulating nucleons, such as proton and neutron. Low-energy electrons are often taken as “by-products” when preparing these nucleons by ionizing atoms, molecules and solids, and high-energy electrons or β rays are taken as “wastage” generated in nuclear reaction. Utilization of those “by-products” has not won sufficient attention from the nuclear physics community. In this chapter, we point out a potential, valuable utilization of those “by-products.” Based on a universal principle of achieving powerful mono-color radiation source, we propose how to set up an efficient powerful electron-based gamma-ray source through available solid-state components/elements. Larger charge-to-mass ratio of an electron warrants the advantage of electron-based gamma-ray source over its nucleon-based counterpart. Our technique offers a more efficient way of manipulating nuclear matter through its characteristic EM stimulus. It can warrant sufficient dose/brightness/intensity and hence an efficient manipulation of nuclear matter. Especially, the manipulation of a nucleus is not at the cost of destroying many nuclei to generate a desired tool, that is, gamma ray with sufficient intensity, for achieving this goal. This fundamentally warrants a practical manipulation of more nuclei at desirable number.

Keywords: gamma-ray source, electron oscillation, DC fields

1. Introduction

Powerful mono-color gamma-ray source is a very appealing, but also seem-to-be-dream, topic in modern physics. This is because the gamma ray, an electromagnetic (EM) wave with sub- pm -level wavelength λ , is generated from quantum transition of nuclear matter in nuclear reaction. At present, using synthesized radioactive heavy elements, or radioisotope, is the main route for achieving a gamma-ray source [1–4]. Finite proton number in a radioactive heavy element is the bottleneck affecting the intensity and power of the gamma-ray output. Higher proton number is favorable not only to higher intensity and power but also faster decay or shorter life of the radioactive heavy element. For practical purposes, such a gamma-ray source should be of a stable output over a sufficiently long time duration. Piling large amount of radioactive heavy elements might be a solution to this requirement but its accompanied environment-protection cost might be overly high. Moreover, because a nucleon has smaller charge-to-mass ratio than an

electron, the accelerator cost and the reactor cost at the synthesis stage are also of considerable amount even though it is only aimed at low-energy nuclear physics applications rather than high-energy physics applications. To some extent, obtaining a powerful mono-color gamma-ray source corresponds to an artful skill of manipulating nuclear matter.

Therefore, new working principle of achieving radiation source with narrower output spectrum is of significant application value. Based on Takeuchi's theory [5], we proposed a universal principle of achieving mono-color radiation source at arbitrary wavelength [6, 7]. According to this principle, available parameter values can ensure a powerful mono-color gamma-ray source.

The core of this working principle can be summarized as "tailoring" Takeuchi orbit. Takeuchi's theory reveals that the orbit of a classical charged particle, such as electron, in a DC field configuration $E_s \times B_s$, where E_s and B_s are constant, can be elliptical or parabolic according to values of E_s and B_s and that of initial particle's velocity entering into this configuration [5, 8]. The time cycle of an elliptical orbit can be in principle an arbitrary value by choosing suitable values of these parameters. Thus, for a far-field observer on the normal direction of this 2-D orbit, electrons moving along the orbit will behave like a radiation source whose central frequency is the inverse of the time cycle of the orbit. But a realistic factor affecting its practicality is the geometric size of such an orbit. Overly large geometric size will hurt the practicality of such a radiation source. At present, for available values of E_s and B_s , about *MV/meter*-level and *Tesla*-level, the size can be down to *m*-level for *s*-level time cycle or *Hz*-level frequency.

For warranting the practicality of such a radiation source, we propose a scheme for making it compact by "tailoring" Takeuchi orbit through targeted designed DC field configuration [6]. In this configuration, B_s is made space-varying along the direction normal to the unperturbed path of an electron bunch by not letting two Helmholtz coils be co-axial on purpose [6]. By choosing suitable values of related parameters, such as the relative distance between the bunch path and the $B_s = 0$ contour, E_s -values and the slope $\beta = d_x B_s$, where B_s is along the y -direction, its magnitude $|B_s|$ is a function of the coordinate x , and the unperturbed path is along the z -axis.

2. Theory and method

2.1 Theoretical basis

For the convenience of readers, we paste related materials published elsewhere [7]. For a simple configuration containing merely static electric field (along x -direction) and static magnetic field (along z -direction), the behavior of an incident electron can be described by dimensionless 3-D relativistic Newton equations (RNEs)

$$d_s[\Gamma d_s Z] = 0, \quad (1)$$

$$d_s[\Gamma d_s Y] = W_B d_s X \quad (2)$$

$$d_s[\Gamma d_s X] = -W_B[\eta + d_s Y] \quad (3)$$

where

$$\frac{1}{\Gamma} = \sqrt{1 - (d_s X)^2 - (d_s Y)^2 - (d_s Z)^2}. \quad (4)$$

Moreover, E_s and B_s are constant-valued electric and magnetic fields and meet $E_s = \eta c B_s$; $\lambda = c/\omega$ and ω are reference wavelength and frequency, respectively; and $s = \omega t$, $Z = \frac{z}{\lambda}$, $Y = \frac{y}{\lambda}$, $X = \frac{x}{\lambda}$, $W_B = \frac{\omega_B}{\omega}$, where $\omega_B = \frac{eB_s}{m_e}$ is the cyclotron frequency.

Eqs. (1)–(3) lead to

$$d_s Z \equiv 0 \quad (5)$$

$$\Gamma d_s Y - W_B X = \text{const} = C_y; \quad (6)$$

$$\Gamma d_s X + W_B [\eta s + Y] = \text{const} = C_x, \quad (7)$$

where the values of these constants, *const*, are determined from the initial conditions $(X, Y, Z, d_s X, d_s Y, d_s Z)|_{s=0} = \left(0, 0, 0, \frac{C_x}{\sqrt{1+C_x^2+C_y^2}}, \frac{C_y}{\sqrt{1+C_x^2+C_y^2}}, 0\right)$.

Eqs. (5)–(7) can yield an equation for $d_s X$ and $d_s Y$

$$(d_s Y)^2 = [C_y + W_B X]^2 * \left[1 - (d_s X)^2 - (d_s Y)^2\right] \quad (8)$$

$$(d_s X)^2 = [C_x - W_B * (\eta s + Y)]^2 * \left[1 - (d_s X)^2 - (d_s Y)^2\right] \quad (9)$$

whose solution reads

$$(d_s X)^2 = \frac{[C_x - W_B * (\eta s + Y)]^2}{\left[1 + [C_y + W_B X]^2 + [C_x - W_B * (\eta s + Y)]^2\right]} \quad (10)$$

$$(d_s Y)^2 = \frac{[C_y + W_B X]^2}{\left[1 + [C_y + W_B X]^2 + [C_x - W_B * (\eta s + Y)]^2\right]}. \quad (11)$$

It is easy to verify that the solutions (10, 11) will lead to

$\Gamma = \sqrt{1 + [C_y + W_B X]^2 + [C_x - W_B * (\eta s + Y)]^2}$ and, with the help of Eqs. (6) and (7), $d_s \Gamma = -W_B \eta * d_s X$ (i.e., $m_e c^2 d_t \Gamma = e E d_t X$). Noting Γ can be formally expressed as $\Gamma = \sqrt{1 + C_y^2 + C_x^2} - W_B \eta * X$, which agrees with Takeuchi's theory [15], we can find that the electronic trajectory can be expressed as

$$\left[\sqrt{1 + C_y^2 + C_x^2} - W_B \eta * X\right]^2 = 1 + [C_y + W_B X]^2 + [C_x - W_B * (\eta s + Y)]^2, \quad (12)$$

or

$$(1 - \eta^2) \left[X + \frac{(\eta + v_{y0})}{1 - \eta^2} \frac{\Gamma_0}{W_B}\right]^2 + \left[(Y + \eta s) - v_{x0} \frac{\Gamma_0}{W_B}\right]^2 = \frac{\left[(\eta + v_{y0})^2 + (1 - \eta^2) v_{x0}^2\right]}{1 - \eta^2} \left(\frac{\Gamma_0}{W_B}\right)^2, \quad (13)$$

where $\Gamma_0 = \sqrt{1 + C_y^2 + C_x^2}$, $v_{x0} = \frac{C_x}{\Gamma_0}$ and $v_{y0} = \frac{C_y}{\Gamma_0}$.

There will be an elliptical trajectory for $\eta < 1$ and a hyperbolic one for $\eta > 1$ [15, 16]. The time cycle for an electron traveling through an elliptical trajectory can be exactly calculated by re-writing Eq. (10) as [15]

$$\pm ds = \frac{\frac{1}{W_B} \Gamma_0 - \eta * X}{\sqrt{aX^2 + bX + c}} dX = \frac{\eta}{\sqrt{-a}} \frac{X_N - X}{\sqrt{\frac{b^2 - 4ac}{4a^2} - \left(X + \frac{b}{2a}\right)^2}} dX, \quad (14)$$

where $a = (\eta^2 - 1)$, $b = -2[\eta\Gamma_0 + C_y] \frac{1}{W_B}$, $c = C_x^2 \left(\frac{1}{W_B}\right)^2$ and $X_N = \frac{1}{\eta} \frac{1}{W_B} \Gamma_0$. The equation can be written as a more general form

$$\pm ds = \sigma \frac{M - u}{\sqrt{1 - u^2}} du \quad (15)$$

where $u = \frac{X + \frac{b}{2a}}{\sqrt{\frac{b^2 - 4ac}{4a^2}}} = \frac{X - \frac{X_R + X_L}{2}}{X_R - X_L}$, $X_L = \min\left(\frac{-b - \sqrt{b^2 - 4ac}}{2a}, \frac{-b + \sqrt{b^2 - 4ac}}{2a}\right)$ and $X_R = \max\left(\frac{-b - \sqrt{b^2 - 4ac}}{2a}, \frac{-b + \sqrt{b^2 - 4ac}}{2a}\right)$. In addition, $\sigma = \frac{\eta}{\sqrt{-a}} \sqrt{\frac{b^2 - 4ac}{4a^2}}$ and $M = \frac{X_N + \frac{b}{2a}}{\sqrt{\frac{b^2 - 4ac}{4a^2}}} = \frac{X_N - \frac{X_R + X_L}{2}}{X_R - X_L}$. It is easy to verify that for $\eta^2 - 1 < 0$, there is $M = \frac{1 + \eta v_{y0}}{\eta \sqrt{(\eta + v_{y0})^2 + (1 - \eta^2) v_{x0}^2}} > 1$.

Initially, $(X, Y)|_{s=0} = (0, 0)$ and hence $u_{st} = u|_{s=0} = \frac{0 + \frac{b}{2a}}{\sqrt{\frac{b^2 - 4ac}{4a^2}}} = \frac{-(\eta + v_{y0})}{\sqrt{(\eta + v_{y0})^2 + (1 - \eta^2) v_{x0}^2}}$.

From strict solution

$$\pm s(u) = \sigma * \left\{ M * \arcsin(u) + \sqrt{1 - u^2} \right\} + const, \quad (16)$$

we can find the time for an electron traveling through an elliptical trajectory to meet $s_{cycle} = \omega T_c = 2 * [\sigma M \pi]$ and hence a time cycle $T_c = \frac{(1 + \eta v_{y0}) \Gamma_0}{(\sqrt{1 - \eta^2})^3 \omega_B} \frac{2\pi}{\omega_B}$. That is, the oscillation along the elliptical trajectory will have a circular frequency ω_B . Moreover, it is interesting to note that $(v_{x0}, v_{y0}) = (0, -\eta)$ will lead to $\frac{[(\eta + v_{y0})^2 + (1 - \eta^2) v_{x0}^2]}{1 - \eta^2} = 0$ and hence a straight-line trajectory $(X(s), Y(s)) = (0, -\eta s)$.

The motion on an elliptical trajectory is very inhomogeneous. The time for finishing the $\eta X > 0$ half might be very short while that for the $\eta X < 0$ half might be very long. We term the two halves as fast-half and slow-half, respectively. If η is fixed over whole space, a fast-half is always linked with a slow-half and hence makes the time cycle for finishing the whole trajectory being at considerable level.

For convenience, our discussion is based on the parameterized ellipse. For the case $(v_{x0} = 0, v_{y0} = -\eta - \Delta)$, (where Δ is small-valued and positive), the starting position $X = 0$ is the left extreme of the ellipse and hence corresponds to $u = -1$. The time required for an acute-angled rotation from $u = -1$ to $u = -1 + \xi$, (where ξ is small-valued and positive), will be $\sigma M * [\arcsin(-1 + \xi) - \frac{\pi}{2}] + \sigma \sqrt{2\xi - \xi^2}$, which is $= 0$ if $\xi = 0$.

It is interesting to note that if there is $B = 0$ at the region $u > -1 + \xi$, the electron will enter from $(E, B = \frac{E}{\eta c})$ -region into $(E, B = 0)$ -region with an initial velocity whose x -component is $v_{x1} \sim d_s u|_{u=-1+\xi} = \frac{1}{\sigma} \frac{\sqrt{1 - (-1 + \xi)^2}}{M - (-1 + \xi)} > 0$ and y -component v_{y1} is $\neq 0$. Then, the electron will enter into the $(E, B = 0)$ -region at a distance because $v_{x1} > 0$. After a time $T_{tr} = \frac{2v_{x1}}{E \sqrt{1 - v_{x1}^2 - v_{y1}^2}}$, the electron will return into the $(E, B = \frac{E}{\eta c})$ -region and the returning velocity will have a x -component $-v_{x1}$. During

this stage, the electron will move $v_{y1} * T_{tr}$ along the y direction. Then, the motion in the $(E, B = \frac{E}{\eta c})$ -region can be described by an acute-angled rotation along the ellipse $u = -1 + \xi \rightarrow u = -1$. Thus, a complete closed cycle along the x direction is finished even though the motion along the y direction is not closed. Repeating this closed cycle will lead to an oscillation along the x direction.

Clearly, the time cycle of such an oscillation, or that of a “tailored” Takeuchi orbit, is

$$T_x = T_{tr} + 2\sigma M * \left[\arcsin(-1 + \xi) - \frac{\pi}{2} \right] + 2\sigma \sqrt{2\xi - \xi^2}. \quad (17)$$

Under fixed values of Δ , E and B , the smaller ξ is, the smaller T_x is. There will be $T_x = 0$ at $\xi = 0$. In principle, arbitrary value of $T_x < T_c$ can be achieved by choosing suitable value of ξ . That is, arbitrarily high center frequency ($> \omega_B$) oscillation can be achieved by choosing a suitable value of ξ . Although the time history of $x(t)$ might cause its Fourier spectrum to have some spread, the center frequency will be $\frac{1}{T_x}$.

This result implies a simple and universal method of setting up quasi-mono-color light source at any desirable center wavelength: by applying vertically static electric field $E = E_x$ and static magnetic field $B = B_z$ and on purpose letting a $B = 0$ region exist and the ratio $\frac{E}{cB} < 1$, then injecting electron along the y -axis with a velocity slightly above $|\frac{E}{cB}|$, and close to the boundary line between the $B = 0$ region and the $B \neq 0$ region. As shown in **Figure 1** of Ref. [7], adjusting the distance $D = \xi * \sqrt{\frac{b^2 - 4ac}{4a^2}}$ can lead to a quasi-monocolor oscillation source with any desired center frequency up to gamma-ray level.

Of course, such a step-like magnetic field profile is overly idealized. Therefore, we propose using a more realistic magnetic slope to achieve such a tailored Takeuchi orbit [6].

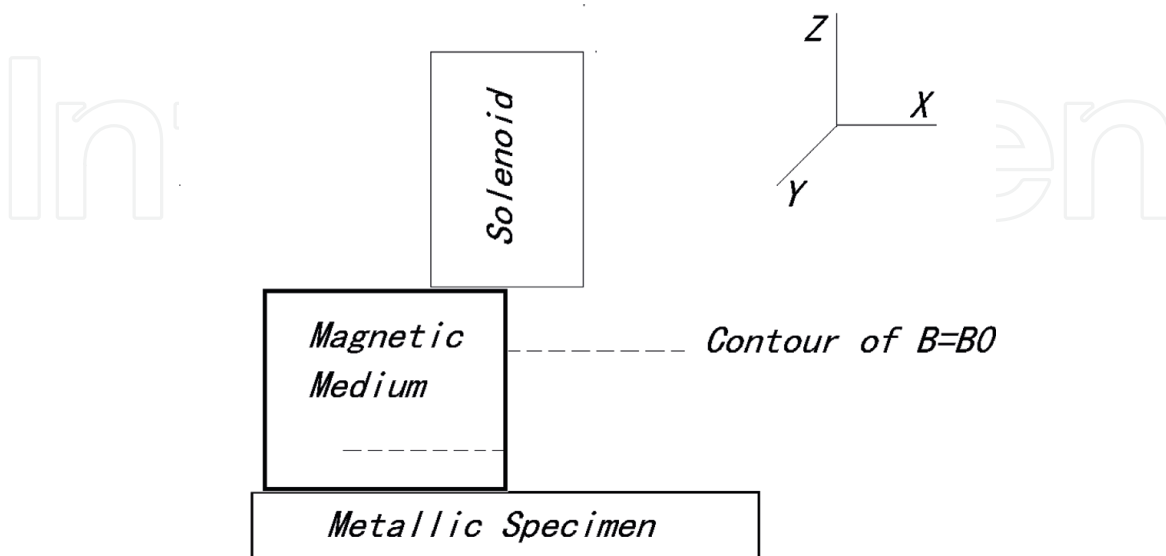


Figure 1. Sketch of the device. The axis of a finite-sized solenoid is along z direction, the space between the solenoid and the conducting wire/specimen is filled with two kinds of magnetic mediums, which are represented by μ_{high} and μ_{low} . The μ_{low} medium can be the vacuum. A pair of electrodes yields a DC electric field along the x direction on the specimen. The dashed line represents the contour plane of B at a given value B_0 . Different μ values cause the contour plane to have different z coordinates in two mediums.

2.2 Details on electron source

The above discussions have revealed theoretically the feasibility of an electron oscillation-based gamma-ray source. It is obvious that the electron oscillation-based radiation source is more advantageous than its proton oscillation-based counterpart because of larger oscillation magnitude, as well as power, available in the former. Utilization of electrons receives less attention than that of protons in experimental nuclear physics. It is really a pity if taking electrons as by-products of preparing protons. Reasonably utilizing those “by-products” is worthy of consideration.

Electron source can be designed to be compact and easily prepared. Among familiar electron sources, thermion-emission cathode is limited by its efficiency, and photocathode needs to be driven by high-intensity laser. The simplest method of achieving a high-efficiency electron source can share the same idea as that embodied in above sections, that is, using Hall effect by a magnetic slope in the above-mentioned discussion. Details are presented as follows.

Hall effect of a metal by a static (DC) magnetic field B_s is a familiar phenomenon caused by magnetic field. But until now, it is merely taken as a method of probing physical property of solid-state materials and hence its applications are often limited to weak magnetic field cases, which are usually at 10G-level. Higher strength of B_s needs stronger strength of current which might be beyond what a conducting wire can sustain and also is far beyond what most magnetic materials can produce [9].

Beside the strength of $|B_s|$, the space shape of B_s can also affect its interaction with matter. Such a space shape is described by the contour surface of B_s . For most components, their generated fields are usually of smooth contour surfaces. For example, B_s generated by a solenoid has contour planes normal to the axis of the solenoid, or the electromagnetic (EM) energy density profile $|B_s|^2$ is smooth or has a very small gradient $\nabla|B_s|^2$.

If the strength $|B_s|$ is not easy to be enhanced, adjusting the space shape of B_s is a worthy trial to optimize interaction. A high-gradient $|B_s|^2$ profile is not difficult to be produced. For example, one can on purpose make a pair of Helmholtz coils, which is a well-known device for screening external magnetic field, so that they are not co-axial. **Figure 1** displays a simple scheme for producing a high-gradient $|B_s|^2$ profile. As shown in **Figure 1**, the intrusion of a high- μ (magnetic permeability) medium distorts contours of $|B_s|^2$ to be bent. In other words, in each plane normal to the axis of the solenoid, a huge gradient of $|B_s|^2$ along the direction normal to the side surface of the medium appears. If a metal wire/specimen is arranged in such a high- $\nabla|B_s|^2$ region and an DC electric field E_s along the direction of $\nabla|B_s|^2$ is applied, the Hall effect in such a situation where the DC magnetic field is very space-inhomogeneous is worthy of being studied.

When studying applications such as probing and imagining local magnetic moment and magnetic microscopic structure [10–20], many authors have made in-depth investigation on the Hall effect of semiconductors in highly inhomogeneous magnetic field (HIMF). Because the purpose of these applications is detection or probing, the electric field or bias DC field is designed to avoid the breakdown of the semiconductor and hence its strength is usually not too strong. That is, in applications for detection purpose, Hall current is not required to be large enough.

It is worth noting the potential value of the extension of the same idea to a different case. The purpose of such an extension is aimed at a controllable “break-down” of the metal. Therefore, higher DC field strength is chosen. Now that Hall effect implies that electrons have the potential to run along a direction normal to the

applied electric field, it is natural for us to consider the feasibility of side escape of electrons from a conducting wire through Hall effect. This drives us to actively establish a HIMF and apply it to metal under a higher-strength DC electric field.

E_s can achieve 10^5V/m -level by letting the inter-plate distance of a pair of plane-plate electrodes as $10^{-3} \sim 10^{-2} \text{m}$ and applied voltage as $10^{2 \sim 3} \text{V}$. Parameter values at such a level is not difficult to be realized technically. Because of the condition $\nabla \cdot B = 0$ and the fact that the solenoid is finite-sized, B_s has two components $B_x \vec{e}_x$ and $B_z \vec{e}_z$, where $B_x = \sum_i g x_i x_i^{2i+1}$ and $B_z = \sum_i g z_i x_i^{2i+1}$ correspond to a vector potential $\vec{A} = A_x \vec{e}_x + A_z \vec{e}_z = -y B_z \vec{e}_x + y B_x \vec{e}_z$.

As shown in **Figure 1**, the solenoid is arranged on the demarcation line of two magnetic mediums. The end section of the solenoid is taken as the $z = 0$ plane, and the metal is arranged at $z < -|z_d|$ region. The $(x < 0, |z_u| > z > -|z_d|)$ region is filled with $\mu = \mu_{high}$ medium and the $(x > 0, |z_u| > z > -|z_d|)$ region with $\mu = \mu_{low}$ medium. According to the theory of electromagnetism, the contour plane $B_z = B_0$ in the $(x < 0, -|z_d| > z)$ region and that in the $(x > 0, -|z_d| > z)$ region will have different z coordinates. This implies a discontinuity in B exists near the demarcation line. That is, different values of the dropping rate $\partial_z |B|$ in two mediums cause the specimen in the $(-|z_d| > z)$ region to still feel a gradient $\partial_x |B|^2$. To ensure a sufficiently large gradient, the interface of two mediums is required to be smooth enough and hence should be polished/ground sufficiently. At present, mirror finish grinding can ensure surface roughness to be of $Ra \leq 0.01 \mu\text{m}$. This fundamentally warrants sufficiently large gradient $\partial_x \mu$, as well as sufficiently large $\partial_x B^2$ up to $\frac{T}{nm}$ -level, to be feasible.

Because the DC magnetic field can effectively penetrate into metal interior if its direction is normal to the surface of a metal (in normal state), it can affect bulk electron states of the metal. In contrast, the AC magnetic field, or a light beam, is limited to the skin layer of the metal [21, 22].

For *Al*, its electron-phonon collision relaxation time τ is at $10^{1 \sim 2} \text{fs}$ -level [21, 22], its Fermi velocity v_F is at 10^6m/s -level and its Fermi energy E_F is about 5.5eV [21, 22]. If a cm^3 -level *Al* cubic specimen is placed between a pair of electrode plates with 220V voltage, the DC electric field E_s it feels will be at 10^4V/m -level. If we merely take into account the work done by E_s , the maximum velocity increment along the E_s direction, $\max \Delta v_x$, can reach $e E_s \tau / m_e = 1.6 / 9.1 * 10^{-19+4-15+1+31} \approx 20 \text{m/s}$, which corresponds to $\frac{1}{2} m_e v_x^2 \sim 200 * 9.1 * 10^{-31} \text{J} \approx 10^{-9} \text{eV}$.

Emission is a many-body process because the sheath field, or space charge effect, left by emitted electrons in turn affects emission [23–26]. This phenomenon can be reflected by following quantum theory (21, 23–26),

$$i \hbar \partial_t \psi_k = \frac{1}{2m_e} [i \hbar \nabla + e B_0 y \vec{e}_x]^2 \psi_k + U_i \psi_k + V(x, y) \psi_k + e E_0 x \psi_k + V_{ph}(x, y, t; T) \psi_k. \quad (18)$$

$$\nabla^2 V = \frac{e}{4\pi \epsilon_0} n_0 \left(1 - \frac{\int \int |\psi_k|^2 f(k, T) dk_x dk_y}{n_0} \right) \quad (19)$$

where

$$V_{ph} = \iint [\vec{u}_q \cdot \nabla_r U_i] g(k, T) dq_x dq_y, \quad (20)$$

$$\vec{u}_q = \sin(q_x x + q_y y + q_z z - \nu_q t) \vec{e}_p, \quad (21)$$

n_0 is the average background ionic density, $\psi_k(x, y, t) = \exp(S_k)\psi_k^0$, ψ_k^0 is the unperturbed wavefunction and f is the Fermi-Dirac distribution function. V_{ph} is the vibrating lattice potential, u is the field of ionic displacement, U_i is the lattice potential at zero-temperature, g is the Bose-Einstein distribution function, ν_q is the phonon dispersion relation and T is the temperature. More comprehensive model should contain a motion equation of the displacement field u , which is derived from the Lagrangian density of the electron-phonon system. This will be done in future work. Here, we approximate u as prescribed. Such an approximation is acceptable because the temporal variation of u is merely obvious over a large time scale $\frac{2\pi}{\nu_q}$ which is usually $> 100fs$.

The equation of S_k reads

$$\begin{aligned} i\hbar\partial_t S_k = & -\frac{\hbar^2}{2m_e} \left[(\partial_{xx} + \partial_{yy} + \partial_{zz})S_k + (\partial_x S_k)^2 + (\partial_y S_k)^2 + (\partial_z S_k)^2 \right] \\ & + 2ik_x \partial_x S_k + 2ik_y \partial_y S_k + 2ik_z \partial_z S_k \\ & - \frac{\hbar B_0}{m_e} ey(k_x f_x - k_z f_z) + \frac{i\hbar B_0}{m_e} ey(f_x \partial_z - f_z \partial_x) S_k \\ & + \frac{e^2 B_0^2 (f_x^2 + f_z^2)}{2m_e} y^2 + eE_0 x + V(x, y) + V_{ph}, \end{aligned} \quad (22)$$

where the space inhomogeneity of B_s is reflected by f

$$f = (f_x, 0, f_z) = (B_x/B_0, 0, B_z/B_0). \quad (23)$$

Note that $f = (0, 0, 1)$ corresponds to a space-homogeneous $B_s = B_0$ along z direction.

Actively applying highly space-inhomogeneous external field, especially DC magnetic field, might be an effective way of enhancing the effect of the external field on the electrons. According to Hamiltonian formula or Eq. (22), there is always an operator $A \cdot \hat{p} \sim Br\nabla$. Space-inhomogeneous B will cause more space-inhomogeneous wavefunction than space-uniform B . Because the energy of an electron is also dependent on the space derivative of the modulus of its wavefunction, more space-inhomogeneous wavefunction often implies larger energy.

To warrant the technique route to be competitive in economics and efficiency among all candidates for a same goal, we avoid more intermediate conversion steps in EM energy utilization, and favor direct usage of EM energy in power frequency (PF), the most primitive EM energy form for all physics laboratories.

3. Conclusion

The application value of such an electron oscillation-based gamma-ray source is obvious. It offers a more efficient way of manipulating nuclear matter through its characteristic EM stimulus, that is, gamma ray. At present, the goal of manipulating nuclear matter is mainly achieved through: (1) using Bremsstrahlung by proton output from accelerators—this implies the application of an EM stimulus of a broad spectrum to the nucleus, and hence the efficiency of this route is poor because most photons are of low frequency relative to nuclear matter; (2) using EM radiations

from heavier radioactive elements—the dose, or the brightness, or the intensity of gamma ray generated in this route is limited and hence the manipulation is also less efficient; (3) injecting protons into target nucleus. In contrast, the electron oscillation-based mono-color gamma-ray source proposed in this work can warrant sufficient dose/brightness/intensity and hence an efficient manipulation of nuclear matter. Especially, the manipulation of a nucleus is not at the cost of destroying many nuclei to generate a desired tool, that is gamma ray with sufficient intensity, for achieving this goal. This fundamentally warrants a practical manipulation of more nuclei at desirable number.

IntechOpen


IntechOpen

Author details

Hai Lin*, ChengPu Liu and Chen Wang
State Key Laboratory of High Field Laser Physics, Shanghai Institute of Optics and Fine Mechanics, Shanghai, China

*Address all correspondence to: linhai@siom.ac.cn

IntechOpen

© 2019 The Author(s). Licensee IntechOpen. This chapter is distributed under the terms of the Creative Commons Attribution License (<http://creativecommons.org/licenses/by/3.0>), which permits unrestricted use, distribution, and reproduction in any medium, provided the original work is properly cited. 

References

- [1] Hamilton JH. Radioactivity in Nuclear Spectroscopy. Vol. 1. New York: Gordon and Breach; 1972
- [2] Lederer CM, Shirley VS. Table of Isotopes. 7th ed. New York: John Wiley & Sons Inc; 1978
- [3] Sparks P. Handbook of Radioisotopes. New York: NY Reaserch Press; 2015
- [4] Chaudri MA. IEEE Transactions on Nuclear Science. 1975;26:2281
- [5] Takeuchi S. Relativistic $E \times B$ acceleration. Physical Review E. 2002; 66:037402
- [6] H Lin. Monocolor radiation source based on low-energy electron beam and DC fields with high gradient of electromagnetic energy density. Journal of Lasers, Optics and Photonics. 2017;4. DOI: 10.4172/2469-410X.1000161
- [7] H Lin. A simplified and universal setup of quasimonocolor gamma ray source, arXiv. 1503.00815
- [8] Lin H. Miniaturization of solid-state accelerator by compact low-energy-loss electron reflecting mirror. Europhysics Letters. 2015;109:54004
- [9] Strnat KJ. Handbook of Magnetic Materials. Vol. 41988. Elsevier; p. 137
- [10] Bending SJ, Local magnetic probes of superconductors. Advances in Physics. 1999;48:449
- [11] Bending SJ, Oral A. Hall effect in a highly inhomogeneous magnetic field distribution. Journal of Applied Physics. 1997;81:3721
- [12] Thiaville A et al. Measurement of the stray field emanating from magnetic force microscope tips by Hall effect microsensors. Journal of Applied Physics. 1997;82:3182
- [13] Peeters FM, Li XQ. Hall magnetometer in the ballistic regime. Applied Physics Letters. 1998;72:572
- [14] Nabaei V et al. Optimization of Hall bar response to localized magnetic and electric fields. Journal of Applied Physics. 2013;113:064504
- [15] Veracke K et al. Size dependence of microscopic Hall sensor detection limits. Review of Scientific Instruments. 2009; 80:074701
- [16] Engel-Herbert R, Schaadt DM, Hesjedal T. Analytical and numerical calculations of the magnetic force microscopy response: A comparison. Journal of Applied Physics. 2006;99: 113905
- [17] Liu S et al. Effect of probe geometry on the Hall response in an inhomogeneous magnetic field: A numerical study. Journal of Applied Physics. 1998;83:6161
- [18] Koon DW, Knickerbocker CJ. What do you measure when you measure the Hall effect? Review of Scientific Instruments. 1993;64:510
- [19] Comelissens YG, Peeters FM. Response function of a Hall magnetosensor in the diffusive regime. Journal of Applied Physics. 2002;92: 2006
- [20] Folks L et al. Near-surface nanoscale InAs Hall cross sensitivity to localized magnetic and electric fields. Journal of Physics C. 2009;21:255802
- [21] Ashcroft NW, Mermin ND. Solid State Physics. Orlando: Harcourt. Inc; 1976. p. 5, 36, 37
- [22] Kittel C. Introduction to Solid State Physics. New York: John Wiley Sons; 2005

[23] Lang ND, Kohn W. Theory of Metal Surfaces: Charge Density and Surface Energy. *Physical Review B*. 1970;**1**:4555

[24] Jensen KL. General formulation of thermal, field, and photoinduced electron emission. *Journal of Applied Physics*. 2007;**102**:024911

[25] Jensen KL. Exchange-correlation, dipole, and image charge potentials for electron sources: Temperature and field variation of the barrier height. *Journal of Applied Physics*. 1999;**85**:2667

[26] Rokhlenko A, Jensen KL, Lebowitz JL. *Journal of Applied Physics*. 2010;**107**:014904

IntechOpen